Article

The Mechanism for the Rhodium-Catalyzed Decarbonylation of Aldehydes: A Combined Experimental and Theoretical Study

Peter Fristrup, Michael Kreis, Anders Palmelund, Per-Ola Norrby, and Robert Madsen

J. Am. Chem. Soc., **2008**, 130 (15), 5206-5215 • DOI: 10.1021/ja710270j • Publication Date (Web): 28 February 2008

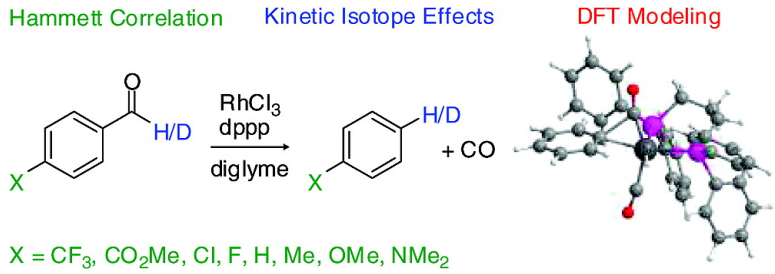

More About This Article

Additional resources and features associated with this article are available within the HTML version:

- Supporting Information
- Links to the 2 articles that cite this article, as of the time of this article download
- Access to high resolution figures
- Links to articles and content related to this article
- Copyright permission to reproduce figures and/or text from this article

View the Full Text HTML

J|A|C|S
ARTICLES

Published on Web 02/28/2008

The Mechanism for the Rhodium-Catalyzed Decarbonylation of Aldehydes: A Combined Experimental and Theoretical Study

Peter Fristrup,[†] Michael Kreis,[†] Anders Palmelund,[†] Per-Ola Norrby,[‡] and Robert Madsen*[,†]

Center for Sustainable and Green Chemistry, Department of Chemistry, Building 201, Technical University of Denmark, DK-2800 Lyngby, Denmark, and Department of Chemistry, University of Gothenburg, Kemigården 4, SE-412 96 Göteborg, Sweden

Received November 13, 2007; E-mail: rm@kemi.dtu.dk

Abstract: The mechanism for the rhodium-catalyzed decarbonylation of aldehydes was investigated by experimental techniques (Hammett studies and kinetic isotope effects) and extended by a computational study (DFT calculations). For both benzaldehyde and phenyl acetaldehyde derivatives, linear Hammett plots were obtained with positive slopes of +0.79 and +0.43, respectively, which indicate a buildup of negative charge in the selectivity-determining step. The kinetic isotope effects were similar for these substrates (1.73 and 1.77 for benzaldehyde and phenyl acetaldehyde, respectively), indicating that similar mechanisms are operating. A DFT (B3LYP) study of the catalytic cycle indicated a rapid oxidative addition into the C(O)−H bond followed by a rate-limiting extrusion of CO and reductive elimination. The theoretical kinetic isotope effects based on this mechanism were in excellent agreement with the experimental values for both substrates, but *only* when migratory extrusion of CO was selected as the rate-determining step.

Introduction

Reactions involving transfer of carbon monoxide via transition metals (carbonylation,[1] hydroformylation,[2] and decarbonylation) belong to the very heart of organometallic chemistry, but to our knowledge, only the two former have been studied by computational methods—presumably owing to their established industrial importance. As part of a continued effort toward the development of more sustainable chemical transformations and, in particular, the utilization of bioderived starting materials in organic synthesis, we have turned our attention toward the rhodium-mediated decarbonylation.[3] In its stoichiometric form, the reaction was discovered by Tsuji and Ohno in 1965,[4] and a couple of years later an increase in temperature allowed substoichiometric amounts of the metal catalyst to be used.[5]

In the more than 40 years that have passed since the discovery of the reaction, there has been an ongoing interest in the development of the methodology[6] as well as its application in synthesis.[7,8] Significant progress toward a more efficient decarbonylation methodology was achieved by Doughty and Pignolet in 1978 through the introduction of chelating bisphosphines as ligands for rhodium.[9] The favored catalyst was found to be [Rh(dppp)$_2$]Cl, and this advancement was followed by a

[†] Technical University of Denmark.
[‡] University of Gothenburg.

(1) Monsanto process (carbonylation of methanol): (a) Cheong, M.; Ziegler, T. *Organometallics* **2005**, *24*, 3053–3058. (b) Feliz, M.; Freixa, Z.; van Leeuwen, P. W. N. M.; Bo, C. *Organometallics* **2005**, *24*, 5718–5723. (c) Daura-Oller, E.; Poblet, J. M.; Bo, C. *Dalton Trans.* **2003**, 92–98. (d) Kinnunen, T.; Laasonen, K. *J. Organomet. Chem.* **2003**, *665*, 150–155. (e) Cavallo, L.; Solà, M. *J. Am. Chem. Soc.* **2001**, *123*, 12294–12302. (f) Ivanova, E. A.; Gisdakis, P.; Nasluzov, V. A.; Rubailo, A. I.; Rösch, N. *Organometallics* **2001**, *20*, 1161–1174.

(2) Hydroformylation: (a) Sparta, M.; Børve, K. J.; Jensen, V. R. *J. Am. Chem. Soc.* **2007**, *129*, 8487–8499. (b) Gleich, D.; Hutter, J. *Chem.—Eur. J.* **2004**, *10*, 2435–2444. (c) Landis, C. R.; Uddin, J. *J. Chem. Soc., Dalton Trans.* **2002**, 729–742. (d) Carbó, J. J.; Maseras, F.; Bo, C.; van Leeuwen, P. W. N. M. *J. Am. Chem. Soc.* **2001**, *123*, 7630–7637. (e) Alagona, G.; Ghio, C.; Lazzaroni, R.; Settambolo, R. *Organometallics* **2001**, *20*, 5394–5404. (f) Decker, S. A.; Cundari, T. R. *J. Organomet. Chem.* **2001**, *635*, 132–141. (g) Schmid, R.; Herrman, W. A.; Frenking, G. *Organometallics* **1997**, *16*, 701–708.

(3) For a recent review on rhodium-catalyzed C−C bond cleavage reactions, see: Necas, D.; Kotora, M. *Curr. Org. Chem.* **2007**, *11*, 1566–1591.

(4) Tsuji, J.; Ohno, K. *Tetrahedron Lett.* **1965**, 3969–3971.

(5) Ohno, K.; Tsuji, J. *J. Am. Chem. Soc.* **1968**, *90*, 99–107.

(6) (a) Fessard, T. C.; Andrews, S. P.; Motoyoshi, H.; Carreira, E. M. *Angew. Chem., Int. Ed.* **2007**, *46*, 9331–9334. (b) Lee, H. W.; Chan, A. S. C.; Kwong, F. Y. *Chem. Commun.* **2007**, 2633–2635. (c) Beck, C. M.; Rathmill, S. E.; Park, Y. J.; Chen, J.; Crabtree, R. H.; Liable-Sands, L. M.; Rheingold, A. L. *Organometallics* **1999**, *18*, 5311–5317. (d) O'Connor, J. M.; Ma, J. *J. Org. Chem.* **1992**, *57*, 5075–5077. (e) Baldwin, J. E.; Barden, T. C.; Pugh, R. L.; Widdison, W. C. *J. Org. Chem.* **1987**, *52*, 3303–3307.

(7) For recent applications in total synthesis, see: (a) Padwa, A.; Zhang, H. *J. Org. Chem.* **2007**, *72*, 2570–2582. (b) Malerich, J. P.; Maimone, T. J.; Elliott, G. I.; Trauner, D. *J. Am. Chem. Soc.* **2005**, *127*, 6276–6283. (c) Harmata, M.; Wacharasindhu, S. *Org. Lett.* **2005**, *7*, 2563–2565. (d) Weatherhead, G. S.; Cortez, G. A.; Schrock, R. R.; Hoveyda, A. H. *Proc. Natl. Acad. Sci. U.S.A.* **2004**, *101*, 5805–5809. (e) Banwell, M. G.; Coster, M. J.; Edwards, A. J.; Karunaratne, O. P.; Smith, J. A.; Welling, L. L.; Willis, A. L. *Aust. J. Chem.* **2003**, *56*, 585–595. (f) Allin, S. M.; James, S. L.; Elsegood, M. R. J.; Martin, W. P. *J. Org. Chem.* **2002**, *67*, 9464–9467. (g) Kato, T.; Hoshikawa, M.; Yaguchi, Y.; Izumi, K.; Uotsu, Y.; Sakai, K. *Tetrahedron* **2002**, *58*, 9213–9222. (h) Boeckman, R. K., Jr; Zhang, J.; Reeder, M. R. *Org. Lett.* **2002**, *4*, 3891–3894.

(8) For applications in carbohydrate chemistry, see: (a) Monrad, R. N.; Madsen, R. *J. Org. Chem.* **2007**, *72*, 9782–9785. (b) Andrews, M. A.; Gould, G. L.; Klaeren, S. A. *J. Org. Chem.* **1989**, *54*, 5257–5264.

(9) Doughty, D. H.; Pignolet, L. H. *J. Am. Chem. Soc.* **1978**, *100*, 7083–7085.

10.1021/ja710270j CCC: $40.75

mechanistic study, which resulted in a proposal comprising five elementary steps: (i) coordination of the aldehyde, (ii) oxidative addition of the aldehydic C−H bond to form a rhodium−acyl complex, (iii) migratory extrusion of carbon monoxide, (iv) reductive elimination of the product, and (v) dissociation of the extruded carbon monoxide.[10]

Recently, we have developed a more efficient decarbonylation methodology, which relies on the in situ formation of the active catalyst from the commercially available $RhCl_3 \cdot 3H_2O$ and dppp ligand in diglyme as a solvent.[11] This reaction showed good functional group compatibility and, in addition, could be used as part of a tandem Oppenauer oxidation−decarbonylation sequence. In an attempt to discover more efficient catalysts for the decarbonylation, we have undertaken a combined experimental and theoretical study of the existing Rh−dppp system. We believe that a good understanding of the existing system is a necessary prerequisite for performing knowledge-based design of a new catalyst system. During the last decades, the development of computers and algorithms for molecular modeling has allowed the computational chemist to investigate systems of increasing molecular complexity with reasonable accuracy. Here, we incorporate computational chemistry as an integrated part of a mechanistic study directed toward the elucidation of the mechanism for the rhodium-catalyzed decarbonylation.

Results and Discussion

Experimental Study. The experimental part of the mechanistic study will incorporate Hammett studies in line with earlier work,[12] where the observed relative reactivity of different *para*-substituted substrates is used to characterize the selectivity-determining step. Furthermore, the method can be used to differentiate between different mechanistic proposals based on the quality of the fit against different sets of σ values (e.g., "normal", "cationic", or "radical"), which could then serve as a starting point for a computational exploration of the reaction. In addition to the Hammett study, deuterated substrates have been synthesized, allowing for a determination of the kinetic isotope effect, which can be directly compared to a calculated value derived from a theoretical catalytic cycle. In the current study, we have selected a set of *para*-substituted benzaldehydes and envisioned that their relative reactivity could be determined by means of a series of competition experiments.[13] In these experiments, two substrates were decarbonylated simultaneously, and the relative disappearance of the starting material could be quantified using an internal standard (Scheme 1).

Seven different *para*-substituted benzaldehydes that had been found to give good yields with negligible formation of byproduct were included in this study.[11] The decarbonylations were performed in a 0.1 M diglyme solution, which we have shown earlier to be the favored solvent for the reaction.[11] Under these conditions, oxidative addition into the aryl−chloride bond of 4-chlorobenzaldehyde does not occur.[14] Samples were taken at the beginning and at intervals, and the disappearance of both benzaldehyde and the *para*-substituted aldehyde under investigation was quantified by GC relative to the internal standard. Assuming that the two substrates follow the same mechanism, the reaction order in each component will be the same for both substrates in a competition study. If the reaction is first-order in substrate, the relative reactivity can then be obtained as the slope of the line when $\ln(c_0/c)$ for one substrate is plotted against the same values for benzaldehyde. As can be seen in Figure 1, the good linear fit validates the reaction order assumptions.

Scheme 1. Competition Studies for the Decarbonylation of Benzaldehyde versus *p*-Substituted Benzaldehydes

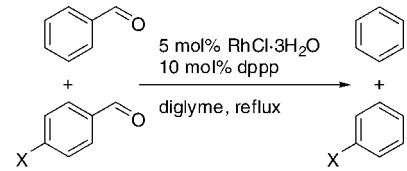

The kinetic data resulted in seven straight lines all with R^2 values above 0.99 (Figure 1). With the slopes of the seven curves, which equal k_X/k_H, the Hammett plot could now be constructed using σ values from the literature (Figure 2).[15] The slope of the line was positive, showing that the reaction is accelerated by electron-withdrawing aldehyde substituents. The observed relative reactivities were in accordance with the "standard" σ values, thus eliminating the possibility of a radical mechanism[12a] which has been shown for the catalytic decarbonylation with transition metal porphyrin complexes.[16]

The relatively small positive slope of +0.79 indicates that a small negative charge is buildup in the transition state (TS) of the selectivity-determining step. This in itself is unsurprising since both oxidative addition and migratory extrusion lead to structures with a carbon−metal bond, thus giving complexes with more negative charge in either the benzylic position or on the aromatic ring. One of the possible methods to differentiate between these two possibilities is a Hammett study of substituted phenyl acetaldehydes. If the selectivity-determining step is the oxidative addition, then there should be no conjugation between the *para*-substituent of the arene and the reacting site, resulting in a low slope for the Hammett plot. If the selectivity-determining step, on the other hand, is the migratory extrusion of carbon monoxide, then the reacting site would be a benzylic position which is in conjugation with the *para*-substituent.

The reactions were carried out under the same conditions as for the benzaldehydes, but because the reactions were too fast, the amount of catalyst had to be reduced to 1.5 mol % (Scheme 2). Again, preliminary studies showed that the reactions of the phenyl acetaldehydes proceeded in quantitative yield with no byproduct formation.

The kinetic data resulted in seven straight lines all with R^2 values above 0.99 (Figure 3). As for the benzaldehydes, electron-withdrawing substituents accelerate the reaction. The resulting Hammett plot is shown in Figure 4.

The linear regression gave a slope of +0.43 but a poorer fit than for the benzaldehydes, with a R^2 of 0.70. While the relative reactivities for the substrates containing non-halide substituents still fall on a reasonable line, the halide-containing phenyl

(10) Doughty, D. H.; Anderson, M. P.; Casalnuovo, A. L.; McGuiggan, M. F.; Tso, C. C.; Wang, H. H.; Pignolet, L. H. *Adv. Chem. Ser.* **1982**, *196*, 65–83.
(11) Kreis, M.; Palmelund, A.; Bunch, L.; Madsen, R. *Adv. Synth. Catal.* **2006**, *348*, 2148–2154.
(12) (a) Keinicke, L.; Fristrup, P.; Norrby, P.-O.; Madsen, R. *J. Am. Chem. Soc.* **2005**, *127*, 15756–15761. (b) Fristrup, P.; Le Quement, S.; Tanner, D.; Norrby, P.-O. *Organometallics* **2004**, *23*, 6160–6165.
(13) (a) Fristrup, P.; Jensen, G. H.; Andersen, M. L. N.; Tanner, D.; Norrby, P.-O. *J. Organomet. Chem.* **2006**, *691*, 2182–2198. (b) Fristrup, P.; Tanner, D.; Norrby, P.-O. *Chirality* **2003**, *15*, 360–368.
(14) A Hammett study by Doughty et al. failed, due to the deactivation of 4-chlorobenzaldehyde in neat solution; see ref 10.
(15) Hansch, C.; Leo, A.; Taft, R. W. *Chem. Rev.* **1991**, *91*, 165–195.
(16) (a) Belani, R. M.; James, B. R.; Dolphin, D.; Rettig, S. J. *Can. J. Chem.* **1988**, *66*, 2072–2078. (b) Domazetis, G.; Tarpey, B.; Dolphin, D.; James, B. R. *J. Chem. Soc., Chem. Commun.* **1980**, 939–940.

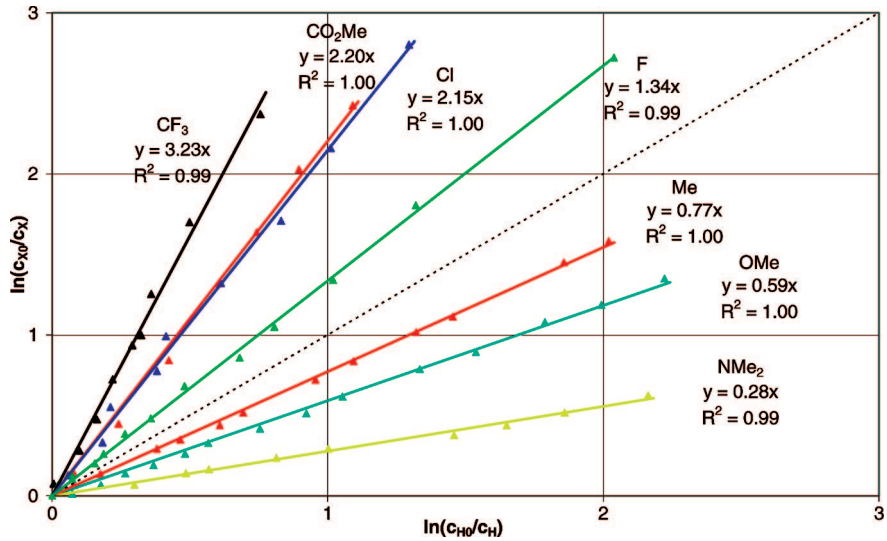

Figure 1. Kinetic data for the decarbonylation of *para*-substituted benzaldehydes.

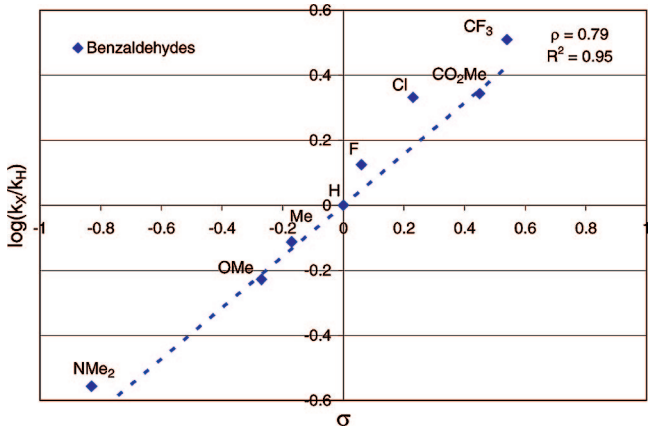

Figure 2. Hammett plot for the decarbonylation of *para*-substituted benzaldehydes.

Scheme 2. Competition Studies for the Decarbonylation of Phenyl Acetaldehydes versus *p*-Substituted Phenyl Acetaldehydes

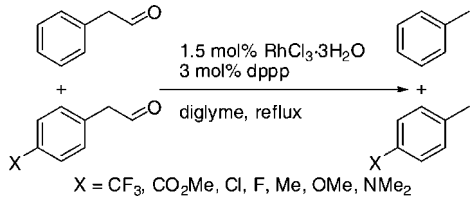

acetaldehydes (F, Cl, and CF_3) reacted faster than would be expected from their σ value. The same tendency was also observed for the benzaldehydes, but it is much less pronounced in that case. To rationalize this, there are two possibilities: either the halide-substituted aldehydes react via a different mechanism or the fit to a single empirical σ_p value is simply not sufficiently accurate. To check the latter possibility, we used the R and F values introduced by Swain and Lupton,[17] which split the σ values into a resonance and an inductive contribution, thereby giving a two-parameter fit. The correlation is, as expected, very much improved, yielding a $R^2 = 0.93$ and a slope of 1.0 with 36% resonance contribution. Similar calculations for the benzaldehydes resulted in a slope of 1.69 with a resonance contribution of 43%. Thus, the substituent influence is weaker for phenyl acetaldehyde, but it is still clear that electrons are shifted toward the aryl ring in the selectivity-determining TS. The lower ρ value for phenyl acetaldehyde is in line with what is expected for introducing a methylene between the aryl ring and the reaction center.[18] Together with the good correlations in Figure 1 and Figure 3, this is an indication that all substrates follow the same reaction mechanism.

We also tested the relative reactivity of benzaldehyde versus that of phenyl acetaldehyde. Somewhat surprisingly, in a direct competition, phenyl acetaldehyde reacted approximately 20 times faster than benzaldehyde, whereas kinetic measurements in separate experiments only gave a factor of 6 in relative reactivity. Thus, the substrate selection includes additional factors beyond the preference in the rate-limiting step, but the difference between these two ratios only corresponds to an energy difference of 3–4 kJ/mol. To see if there is a change in the rate-determining step between the two substrates and to get a better idea whether the oxidative addition or the migratory extrusion is the rate-determining step, we decided to determine the deuterium isotope effect of benzaldehyde and phenyl acetaldehyde. Using 1.5 mol % of $RhCl_3 \cdot 3H_2O$ and 3 mol % of dppp in a comparative kinetic study of benzaldehyde-d_0 or benzaldehyde-d_1, respectively, versus *p*-tolualdehyde, a deuterium isotope effect k_H/k_D of 1.77 was observed for benzaldehyde. For the comparative kinetic study of phenylacetaldehyde-d_0 or phenylacetaldehyde-d_1, respectively, versus 2-(4-methoxyphenyl)acetaldehyde, a deuterium isotope effect k_H/k_D of 1.73 was observed (for further details, see Supporting Information). The similarity of the two kinetic isotope effects indicates that the rate-determining step is the same for both benzaldehyde and phenyl acetaldehyde. The absolute value of the deuterium isotope effect of 1.7–1.8 clearly indicates that the C−H bond has been broken in going from the resting state to the selectivity-determining step. This does not reveal the exact nature of the transition state but is again a strong indication that the C−H bond is intact in the resting state.

Computational Study. To address the ambiguities observed in the experimental study, the investigation was extended with

(17) Swain, C. G.; Lupton, E. C., Jr *J. Am. Chem. Soc.* **1968**, *90*, 4328–4337.

(18) Smith, M. B.; March, J. *March's Advanced Organic Chemistry*, 5th ed.; Wiley: New York, 2001.

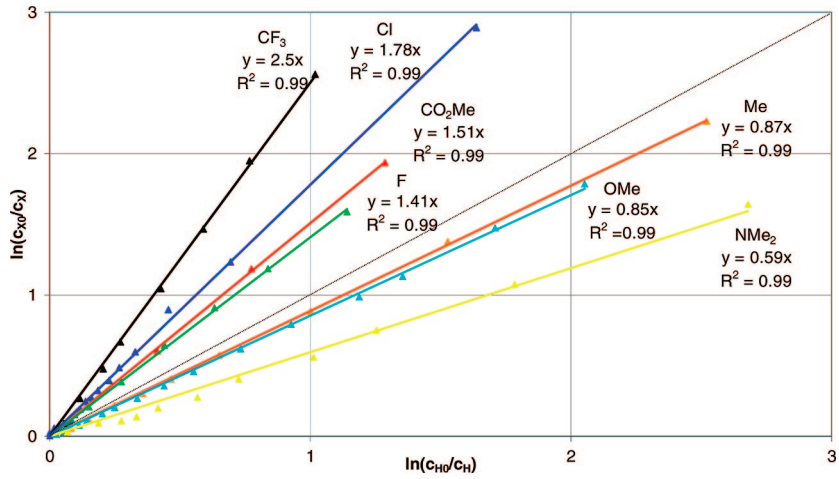

Figure 3. Kinetic data for the decarbonylation of *para*-substituted phenyl acetaldehydes.

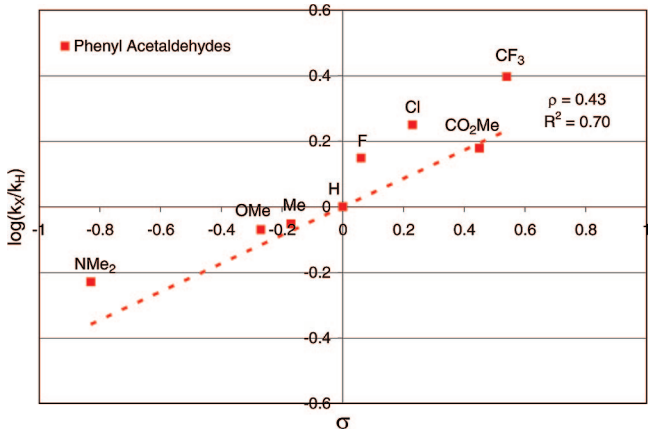

Figure 4. Hammett plot for the decarbonylation of *para*-substituted phenyl acetaldehydes.

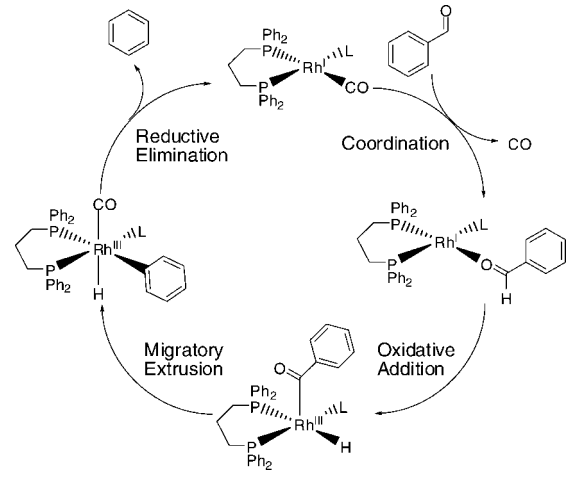

Figure 5. Tentative catalytic cycle for the rhodium-catalyzed decarbonylation of aldehydes.

a computational study. Although recent advances in computing power allow a treatment of the full experimental system, it is often useful to start by investigating a small model system where different mechanistic proposals can be compared within a reasonable time frame. In the present work, the obvious model system consists of a simplified model ligand where the phenyl groups have been removed and replaced by hydrogen. The electronic properties of this model ligand are expected to be reasonably close to those of the real ligand, whereas the reduced size does not offer a possibility for van der Waals and/or electrostatic interactions between the phenyl groups in the substrate and those in the catalyst. However, for the initial evaluation of different mechanistic possibilities, the system should be adequate.

On the basis of the many mechanistic similarities with the rhodium-catalyzed carbonylation and hydroformylation, we suggest a catalytic cycle based on (i) coordination of aldehyde, (ii) oxidative addition, (iii) migratory extrusion, and (iv) reductive elimination as illustrated in Figure 5.

In the original work by Doughty and Pignolet, a catalytic cycle was suggested which contained two dppp molecules per rhodium through the entire cycle. However, calculations performed with the model ligand (Ph = H) indicate that coordination of PhCHO to $Rh(dppp)_2^+$ is highly unfavorable, which were further substantiated by a series of energy minimizations with different fixed distances between Rh^I and the benzaldehyde oxygen atom (distance is varied from 2.7 to 2.0 Å in steps of 0.1 Å, which resulted in an energy increase of about 100 kJ/mol; plot has been included as Supporting Information). Although the model phosphine may not describe the steric interactions accurately, the model is sufficient in this case, where introduction of the additional phenyl groups only leads to an increase of the steric repulsion between the approaching substrate and the Rh^I complex. Instead, we suggest $Rh(dppp)(CO)_2^+$ as a starting point for the catalytic reaction, thus indicating an exchange of CO for PhCHO as the first elementary step. A significant amount of the added catalyst may very well be tied up as $Rh(dppp)_2^+$, CO-bridged dimers, or other low-energy, unreactive resting states, but in the present work, we have focused our attention on the complexes which can be part of the catalytic cycle.

In the coordination chemistry of Rh^I, a square-planar geometry is often preferred, which is also the result achieved when the cationic Rh(model-dppp)$(CO)_2$ complex is optimized using B3LYP/LACVP*. Coordination of the aldehyde takes place via the oxygen atom and gives rise to another square-planar complex which is higher in Gibbs free energy (26 kJ/mol).

Since oxidative addition results in the formation of an additional ligand, there exists the possibility for the generation of three different geometrical isomers of the five-coordinate, octahedral Rh^{III} intermediate. The three different isomers can have either hydride, CO, or the acyl moiety in the apical position

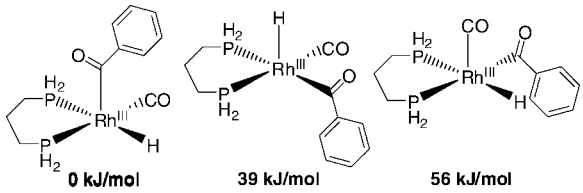

Figure 6. The three possible geometrical isomers of the five-coordinated Rh^{III} intermediate (Gibbs free energies, 298 K).

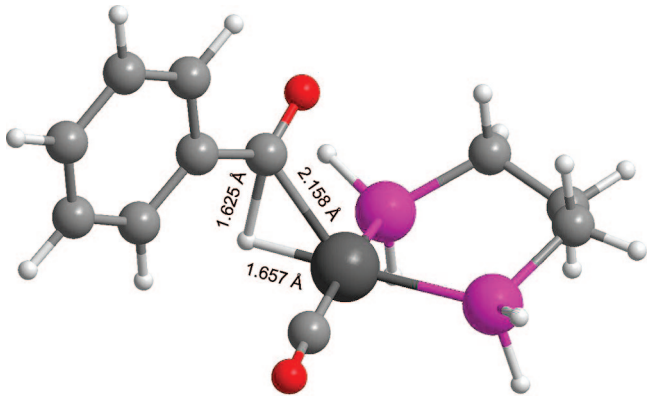

Figure 7. The structure of the transition state for oxidative addition.

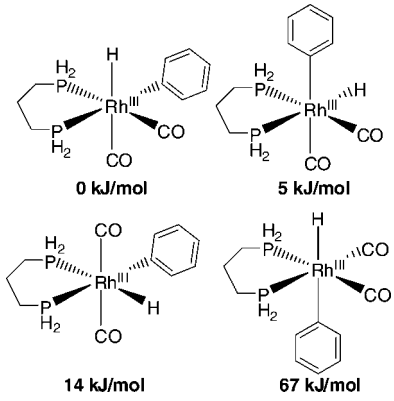

Figure 8. The four possible geometrical isomers of the octahedral Rh^{III} complex (Gibbs free energies, 298 K).

(Figure 6), and since an apical acyl moiety is strongly favored (Figure 6, left), this indicates that the transition state leading to this isomer should also be the most favorable.

The transition state for oxidative addition was found to have a C−H distance of 1.625 Å (Figure 7). This type of three-center TS is ubiquitous in organometallic chemistry.

The next step in the reaction sequence is migratory extrusion of carbon monoxide, which also leads to the occupation of the sixth and last coordination site in the octahedral Rh^{III} complex. Also here, we found it necessary to evaluate several geometrical isomers, and again, we began with the inspection of the octahedral complex formed *after* migratory extrusion. With two identical carbon monoxide ligands, the number of isomers was reduced to four (Figure 8). The two favored isomers both have one of the ligands with the strongest trans-influence (H or Ph) trans to a ligand with weak trans-influence (CO). The structure with both H and Ph trans to phosphines (medium trans-influence) is less favored, and the structure with both ligands with strong trans-influence opposite each other is strongly disfavored.[19]

With such small differences in energy, the influence of the phenyl groups on the ligand may become important, and we will therefore postpone the evaluation of all possible isomers of the transition state for migratory extrusion until the full ligand is included. However, we have located one of the possible transition states (Ph equatorial, H axial, Figure 9) and determined the length of the breaking C−C bond to be 1.838 Å.

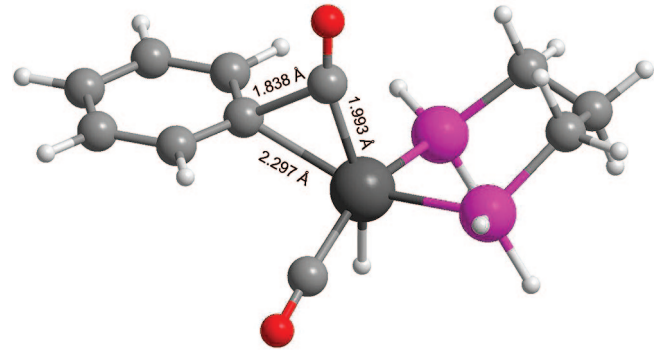

Figure 9. Structure of the transition state for migratory extrusion of carbon monoxide.

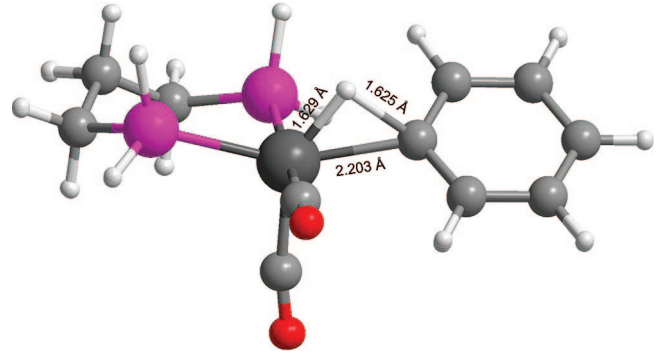

Figure 10. Transition state for reductive elimination of benzene.

After migratory extrusion, the three components originating from the aldehyde (i.e., the "R group", hydride, and CO) take up three coordination sites, but for reductive elimination to take place, the hydride and the phenyl must be in a cis relationship. Again, we anticipate small differences in energy between the isomers with either hydride or phenyl in the apical position and postpone the final evaluation of these isomers. However, employing the model system, we found a transition state for reductive elimination (Figure 10), and the length of the forming C−H bond is 1.625 Å. The elimination of benzene regenerates the $Rh(dppp)(CO)_2$ complex, which is ready to participate in the next catalytic cycle.

Since the dppp ligand occupies two coordination sites and the fragments from the aldehyde a maximum of three (Ph, H, and CO), there will be one additional site available during the entire catalytic cycle (denoted "L" in Figure 5). A priori the identity of this spectator ligand L is unknown, but good candidates would be the ubiquitous carbon monoxide formed during the reaction or the chloride counterion present in the metal precursor ($RhCl_3•3H_2O$). Up until now, we have limited ourselves to CO for simplicity, but we have also investigated the energetics of the entire reaction using chloride, water, or a phosphine as "spectator ligand". To allow a reasonable comparison between the cationic and neutral systems, we have used the PB-SCRF solvation model with parameters suitable for THF.

(19) Appleton, T. G.; Clark, H. C.; Manzer, L. F. *Coord. Chem. Rev.* **1973**, *10*, 335–422.

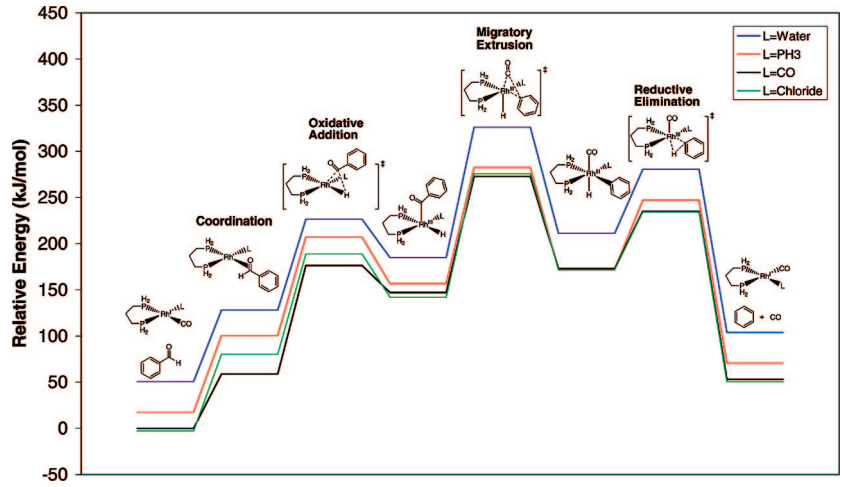

Figure 11. Energy profiles (enthalpy) for four different spectator ligands using the model diphosphine ligand obtained with the solvation model describing THF.

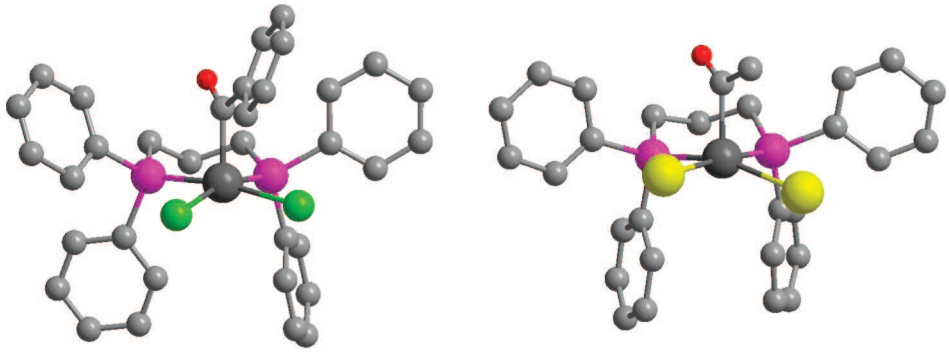

Figure 12. Two X-ray structures of Rh(dppp) complexes illustrating the structure of the five-coordinated Rh^{III} intermediate formed after oxidative addition. Left: Complex with two chlorides and the benzoyl moiety in the apical position. Right: Complex with two iodides and an acetyl moiety in the apical position.

The structures were fully optimized using this solvation model, and the resulting solution phase energies are shown in Figure 11. It is clear that the differences between three of the spectator ligands are insignificant, but the solution phase energy for the water-ligated pathway is constantly ~50 kJ/mol higher than the others. As a consequence, it is therefore difficult to determine the one most likely to be present under experimental conditions, but two of them deserves special notion in this respect. Since chloride is present on rhodium even before formation of the catalytically active species, it may very well stay attached to the metal during the reduction of the Rh^{III} precatalyst to Rh^{I}. In addition, chloride is the only anionic ligand, which should be favorable for coordination to the cationic metal center. In the current study, however, we choose to favor carbon monoxide as a spectator ligand since the abundance of carbon monoxide increases dramatically during the course of the reaction. From these calculations of relative energies, a phosphine ligand also seems plausible; however, these calculations were performed with a model phosphine (PH_3), whereas the real ligand is significantly larger than both chloride and CO and, as a consequence, sterically disfavored.

As suggested originally by Doughty and Pignolet, the additional coordination could also be occupied by another dppp ligand,[9,10] which would dissociate one of the phosphines in the octahedral Rh^{III} intermediate, but as mentioned previously, the approach of benzaldehyde to $Rh(dppp)_2^+$ is strongly disfavored. If the full experimental dppp ligand is included, the combined steric demand forces the complex to adopt a non-square-planar geometry and, as a consequence, renders the approach of an incoming substrate even more difficult.

Computational Study with Full Experimental System: Benzaldehyde. Substitution of the simple hydrogen atoms in the model ligand with phenyl groups dramatically increases the number of possible conformations. However, relevant analogous complexes can be found in the Cambridge Crystallographic Database. The database contains two acyl−rhodium^{III}dppp complexes, depicted in Figure 12 (CCDB codes BZPPRH10 and YIZDIU02). The dppp ligand forms a six-membered chelate, where one side of the ring is blocked by two phenyl groups, whereas the other two phenyl substituents are equatorial, leaving one phase of the metal open. In both structures, the apical acyl ligand is placed on the open face of the catalyst.

With these structures as starting points, we have investigated the decarbonylation of benzaldehyde using DFT calculations (B3LYP functional,[20] LACVP* basis set[21]) in the gas phase. At this level of theory, the decarbonylation of benzaldehyde is exergonic ($\Delta G_{298K} = -8$ kJ/mol). This is attributable to the entropically favored liberation of carbon monoxide, and at even higher temperatures (experimental conditions, $T = 440$ K), the reaction is calculated to be exergonic by 27 kJ/mol. For the

(20) (a) Becke, A. D. *J. Chem. Phys.* **1993**, *98*, 5648–5652. (b) Becke, A. D. *J. Chem. Phys.* **1993**, *98*, 1372–1377. (c) Lee, C.; Yang, W.; Parr, R. G. *Phys. Rev. B* **1988**, *37*, 785–789.

(21) LACVP* uses the 6-31G* basis set for all light elements and the Hay−Wadt ECP and basis set for rhodium; see: Hay, P. J.; Wadt, W. R. *J. Chem. Phys.* **1985**, *82*, 299–310.

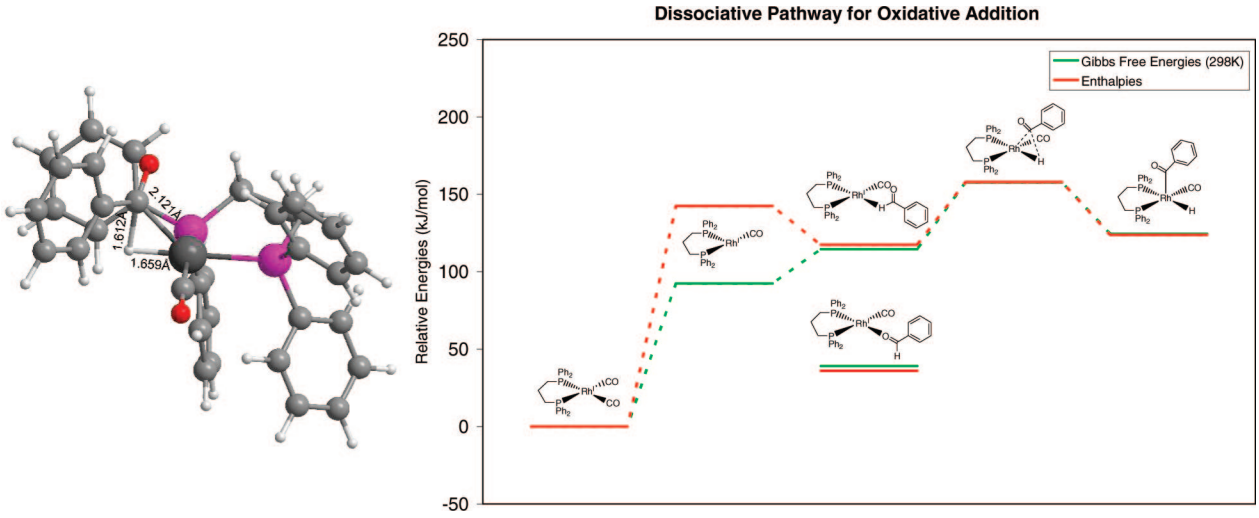

Figure 13. Left: Structure of the transition state for oxidative addition with the reaction taking place in a manner which delivers the acyl moiety to the "open" face of the catalyst. Right: Energy profile for the dissociative pathway.

phenyl acetaldehyde, the decarbonylation becomes more favorable, with calculated Gibbs free energies of 43 and 64 kJ/mol, respectively, at 298 and 440 K. When the selected computational method was applied to an energy minimization of the two X-ray structures depicted in Figure 12, the overall correspondence is good, but the bond lengths to Rh are slightly overestimated in the calculations. Overlaying the metals and directly attached atoms gave an rms deviation of 0.06 Å for BZPPRH10 and 0.16 Å for YIZDIU02, in the latter case mostly due to the overly long Rh−I bonds.

Our starting point and energetic reference was the cationic square-planar $Rh^{I}(dppp)(CO)_2^{+}$ complex. Replacement of one CO by PhCHO leads to a free energy increase of 39 kJ/mol. The dissociative pathway involves expulsion of a CO molecule, leading to the tricoordinated $Rh(dppp)CO^{+}$ complex, which has a higher Gibbs free energy (298 K, 92 kJ/mol), both compared to the $Rh^{I}(dppp)(CO)_2^{+}$ complex. Attempts to identify an associative pathway using the model phosphine were unsuccessful since an approach of benzaldehyde leads to an energy increase as high as 300 kJ/mol without resulting in dissociation of a CO molecule. Benzaldehyde strongly prefers coordination via the oxygen atom, but oxidative addition of the C−H bond requires formation of a prereactive complex with Rh−H coordination (relative Gibbs energy = 114 kJ/mol). From this complex, oxidative addition goes through a three-center transition state with a relative Gibbs free energy of 158 kJ/mol (Figure 13).

The nature of the TS was verified by a full frequency calculation which resulted in a single imaginary frequency of 639 cm^{-1}. After oxidative addition, a five-coordinated intermediate is formed, which has a relative Gibbs free energy of 124 kJ/mol.

The subsequent step in the catalytic cycle is migratory extrusion of carbon monoxide. Of the several possible TSs, only the one leading to a trans relationship between H and Ph could be discarded based on the model studies. The results for the remaining TSs are depicted in Figure 14.

The hydride already present on rhodium prefers a position trans to either phosphorus or spectator carbon monoxide, which can be fulfilled in three of the TSs and results in almost similar energies. These reaction pathways may all be operating under experimental conditions. The TS with hydride positioned trans

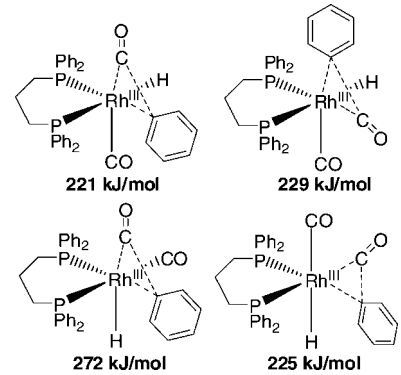

Figure 14. The four isomers for which the migratory extrusion was investigated by DFT calculations.

to the migrating CO moiety can be safely ignored as the barrier was ~50 kJ/mol higher than for the TS with lowest energy.

Backward energy minimizations from the TS revealed the existence of a "preorganized" five-coordinate complex with a free coordination site cis to the acyl moiety. For the lowest energy TS, this complex was characterized and found to have a relative Gibbs free energy of 179 kJ/mol (Figure 15, left).

The transition state for migratory extrusion has a free energy of 221 kJ/mol for the most favored isomer (Figure 15, center, and Figure 16). This TS is very similar to the ones discussed by Ziegler[22] and Cavallo,[23] and in our system, the key distances are C(ipso)−C(O) = 1.928 Å, Rh−C(O) = 1.919 Å, and Rh−C(ipso) = 2.254 Å. The TS was verified by a full frequency calculation which resulted in a single imaginary frequency of 270 cm^{-1}. After migratory extrusion, an octahedral Rh^{III} intermediate is formed with a free energy of 170 kJ/mol. Subsequently, reductive elimination of benzene goes through another three-center TS (Figure 15, right, and Figure 16). Here the barrier is relatively low, only 57 kJ/mol, suggesting that reductive elimination takes place readily after the octahedral Rh^{III} intermediate has been formed. The relative Gibbs free energy of this TS is 227 kJ/mol when compared to the $Rh^{I}(dppp)(CO)_2$ complex, and the key distances are C−H =

(22) Margl, P.; Ziegler, T.; Blöchl, P. E. *J. Am. Chem. Soc.* **1996**, *118*, 5412–5419.
(23) Cavallo, L.; Solà, M. *J. Am. Chem. Soc.* **2001**, *123*, 12294–12302.

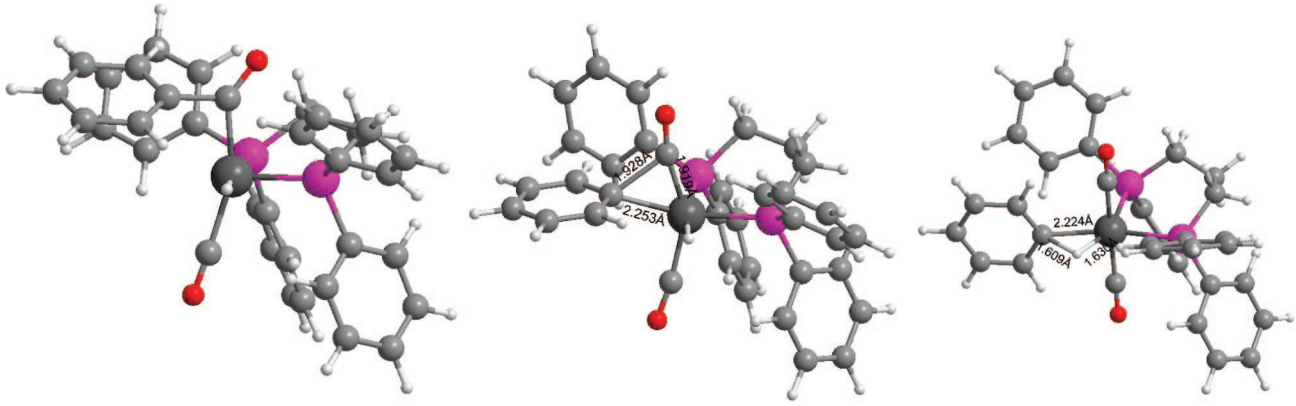

Figure 15. Left: The prereactive complex for the favored isomer of the transition state for migratory extrusion. Center: The favored isomer for the transition state for migratory extrusion. Right: The transition state for reductive elimination of benzene resulting in regeneration of the catalytically active Rh(dppp)$(CO)_2$ complex.

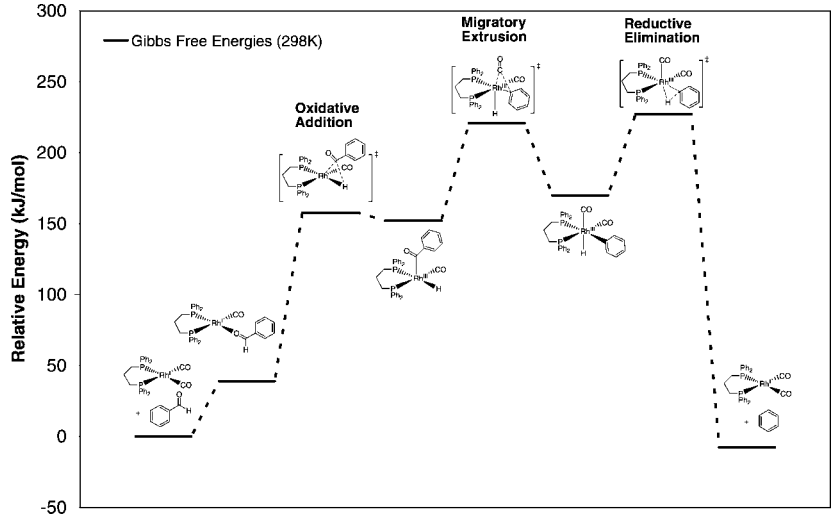

Figure 16. Overview of the catalytic cycle for decarbonylation of benzaldehyde. For clarity, only the isomer having the lowest energy has been included.

1.609 Å, Rh−H = 1.630 Å, and Rh−C = 2.224 Å. The single imaginary frequency was found to be 943 cm^{-1}. Two additional isomers of this TS were found within 1 kJ/mol, and the reaction may therefore very well proceed through several reaction pathways simultaneously. In addition, it can be expected that different substrates could potentially be decarbonylated through different isomeric reaction pathways.

Computational Study with Full Experimental System: Phenyl Acetaldehyde. Although many similarities could be expected between the benzaldehydes and the phenyl acetaldehydes, a thorough computational investigation was still required in order to locate all relevant intermediates for this more flexible substrate. Interestingly, the overall transformation is considerably more favorable for this substrate since the products (toluene and CO) are stabilized by 43 kJ/mol in Gibbs free energy (298 K) compared to the phenyl acetaldehyde starting material (Figure 17).

For this substrate, the initial displacement of CO from the cationic square-planar Rh^{I}dppp$(CO)_2$ is less facile than that for benzaldehyde, resulting in an increase in Gibbs free energy of 57 kJ/mol for the coordination of the aldehyde instead of CO. Again, we expect a dissociative mechanism to be operating. We have not been able to locate a prereactive complex with coordination to the hydrogen atom of the aldehyde functionality as was the case for benzaldehyde. A structure like this is not a stable minimum, but the reaction may still proceed through such a geometry.

It was advantageous to employ the small model phosphine in the initial calculations, but also here the full dppp ligand must be included to achieve a full understanding of the mechanism and energetics of the reaction. In the following discussion, we have limited ourselves to the results obtained using the catalyst with the full dppp ligand.

Oxidative addition takes place through a three-center TS with a relative Gibbs free energy of 152 kJ/mol and a C−H distance of 1.548 Å (Figure 18, left). The two other key bond lengths are 1.681 Å (Rh−H) and 2.109 Å (Rh−C). The identity of the TS was confirmed by a full frequency analysis, which yielded a single imaginary frequency of 629 cm^{-1}. After oxidative addition has taken place, a five-coordinate acyl−Rh^{III} complex is formed with a relative Gibbs free energy of 135 kJ/mol. Also here, the free apical site can be occupied by uptake of an additional CO molecule resulting in a decrease in enthalpy (35 kJ/mol), but a concomitant increase in Gibbs free energy of 20 kJ/mol indicates that this complex is not important under catalytic conditions.

This complex can, in turn, undergo migratory extrusion through a TS with a relative Gibbs free energy of 213 kJ/mol,

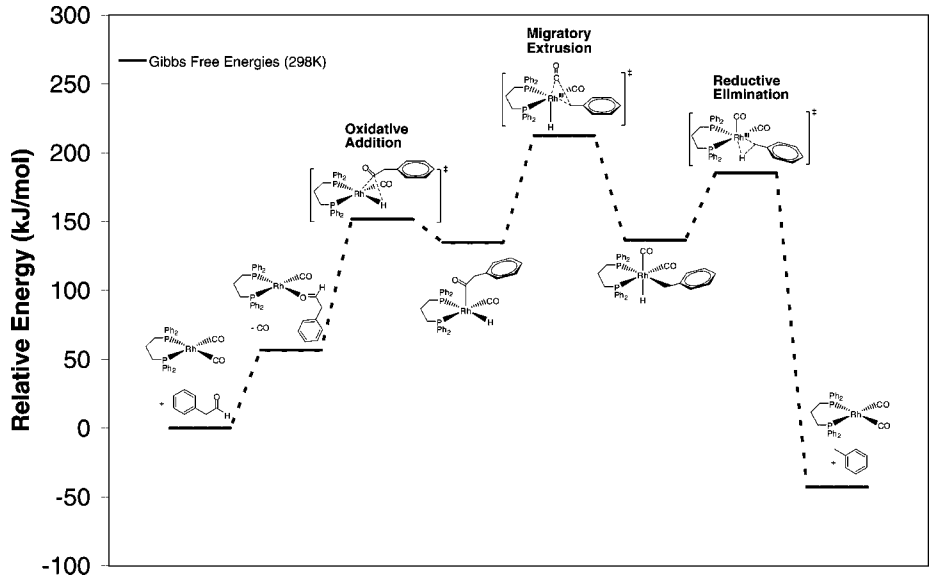

Figure 17. Energy profile for the decarbonylation of phenyl acetaldehyde.

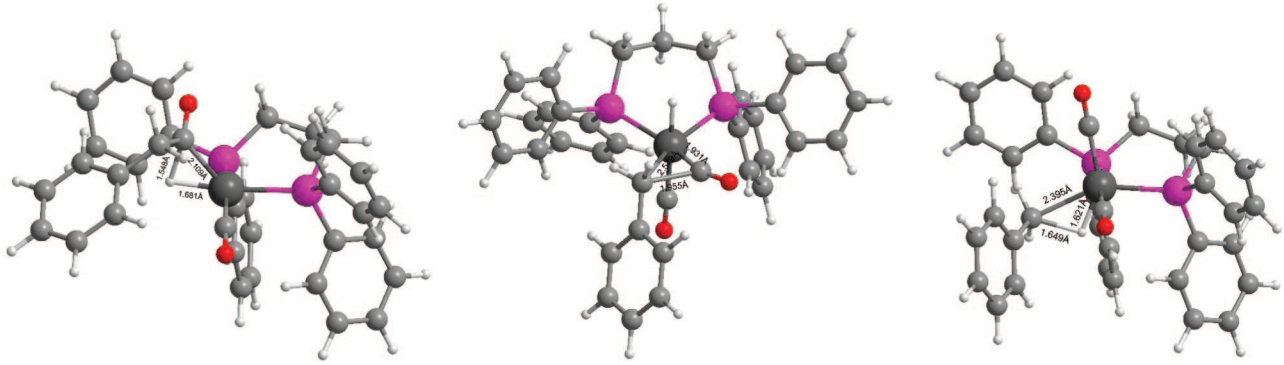

Figure 18. Illustration of the three TSs in the decarbonylation of phenyl acetaldehyde. Left: Oxidative addition into the aldehydic C−H bond. Center: Migratory extrusion of CO to form an octahedral Rh^{III} intermediate. Right: Reductive elimination of toluene, which returns the active $Rh^{I}(dppp)(CO)_2$ complex.

which is 7 kJ/mol lower than that for benzaldehyde (Figure 18, center). Initially, a series of restricted minimizations were carried out with a fixed C−C distance, which revealed that the lowest energy conformation had the two reacting components in an equatorial position. The key distances for the TS geometry are C−C = 1.955 Å, Rh−C(O) = 1.931 Å, Rh−C(benzylic) = 2.579 Å, and the nature of the TS was confirmed by the existence of a single imaginary frequency of 311 cm^{-1}.

After migratory extrusion, an octahedral Rh^{III} complex is formed (relative energy = 137 kJ/mol) from which toluene can be formed by reductive elimination (Figure 18, right). For this process, the activation energy is merely 49 kJ/mol, which results in an early TS with a C−H distance of 1.649 Å. The Rh−H distance is 1.621 Å, whereas the distance from Rh to the benzylic carbon is 2.395 Å. The imaginary frequency was 961 cm^{-1} for this TS.

Although the calculated energy profiles for benzaldehyde and phenyl acetaldehyde are rather similar, there are also differences which deserve attention. As mentioned earlier, in a direct competition experiment, phenyl acetaldehyde reacted about 20 times faster than benzaldehyde, which is in contrast to the results obtained when the two aldehydes are reacted in separate flasks. In this case, there is also a marked difference is reactivity, which results in about 6 times faster conversion of the phenyl acetaldehyde.

The calculated energy profiles can rationalize this difference in reactivity, as the barrier for the rate-determining migratory extrusion is 20 kJ/mol lower for phenyl acetaldehyde. In comparison with the relative reactivities determined experimentally, this difference is obviously too large, but we are satisfied with having captured the correct trend in reactivities and note that an error of about 10 kJ/mol is not surprising when one considers the size of the calculated systems.

For phenyl acetaldehyde, the five-coordinate intermediate is stabilized by 17 kJ/mol compared to the TS for oxidative addition, whereas this intermediate is only stabilized by 6 kJ/mol when benzaldehyde is the substrate. The observed experimental differences between reactions of both substrates, together or in separate flasks, thus give an indication of a catalytic reaction which is not completely governed by Curtin−Hammett conditions. In conclusion, the observed differences in reactivity between benzaldehyde and phenyl acetaldehyde can be explained by the calculated energy profiles, and in addition, the experimental results can be used to pinpoint inaccuracies in the calculated energies.

Deuterium Kinetic Isotope Effect. For benzaldehyde, the experimental kinetic isotope effect (KIE) was determined to be 1.73 (k_H/k_D), whereas for phenyl acetaldehyde, the value was 1.77. The close resemblance for the two different substrates suggests that the same elementary step is rate-determining for

both substrates. A KIE of this magnitude would suggest that the bond to C−H(D) is at least partially broken in the rate-determining step. In the oxidative addition, the C−H(D) bond of the aldehyde is converted to a Rh−H(D) bond, which has a significantly lower stretching frequency (C−H(D) ∼ 2900 (2100) cm^{-1}, Rh−H(D) ∼ 2100 (1500) cm^{-1}).[24] Thus, any of the three types of transition states could be candidates for the rate-limiting step based on the observed KIE. The calculated energy surfaces strongly suggest that either the migratory extrusion or the reductive elimination can be rate-limiting, but for completeness, we have determined theoretical isotope effects for all three types of transition states. The ground state is either the isolated reactants or the catalyst−aldehyde complex. Both options have been tested, but since the two sets of results were virtually identical, only the calculations using the catalyst−aldehyde complex are shown here. As a first crude approximation, we have examined the difference in zero-point energies, which results in a calculated KIE for benzaldehyde of 4.00 at 298 K when oxidative addition is considered to be rate-determining. However, at elevated temperatures, the possibility of populating the excited vibrational states must be included, which is possible using the reduced partition function introduced by Bigeleisen and Mayer,[25] and used for similar systems by, for example, the groups of Houk[26] and Singleton.[27]

The calculation of frequencies and thermodynamic properties for all intermediates and transition states allows the three possibilities to be tested, by simply comparing the calculated KIE at 440 K with the experimentally determined value. With the Rh(dppp)(CO)PhCHO complex as resting state and the assumption that oxidative addition is the rate-determining step, the KIE can be calculated to be 2.85 (k_H/k_D) at 440 K. This value is somewhat higher than the experimental value, and therefore, another scenario was considered where the migratory extrusion is the rate-determining step with the Rh(dppp)(CO)PhCHO complex as a resting state. This resulted in a calculated KIE of 1.80 at 440 K, which is in excellent agreement with the experimental value of 1.73. On the other hand, if reductive elimination is the rate-determining step, the calculated KIE is 2.81, which is almost identical to the value calculated when oxidative addition is rate-determining, and still significantly higher than the experimental value. In those cases where the bond to H(D) is either broken or formed in the rate-determining step, the calculated KIE is too high, whereas for the migratory extrusion where the "probe atom" (i.e., H or D) is not directly involved in the rate-determining elementary step, the calculated KIE is very close to the experimental value. In a similar manner, the KIE for phenyl acetaldehyde was calculated to be 1.79 for the scenario where the resting state is Rh(dppp)CO($PhCH_2CHO$) and the migratory extrusion of CO the rate-determining step. This is in excellent agreement with the experimental value of 1.77, and also here oxidative addition and reductive elimination as the rate-determining steps both lead to higher calculated KIEs of 2.81 and 2.60, respectively.

Conclusion

The mechanism for the rhodium-catalyzed decarbonylation of aldehydes in the presence of a bidentate phosphine ligand (dppp) was investigated by experimental and theoretical methods. All available data indicate that the mechanism consists of oxidative addition, migratory extrusion, and reductive elimination with migratory extrusion as the rate-determining step. The overall good agreement between experiment and theory illustrates that modern theoretical methods have matured to a point where the results can be used to predict and to rationalize experimental results. This opens up the possibility for a number of new applications, such as in silico ligand screening and virtual design of new synthesis routes.

Computational Details

Visualization and comparison of structures were performed in Maestro version 7.5.106.[28] For phenyl acetaldehyde, an initial, simple molecular mechanics conformational search was carried out which resulted in a single conformation with the plane of the phenyl ring and the plane of the C═O moiety arranged perpendicular to each other. DFT calculations were performed with the B3LYP functional[20] employing the LACVP* basis set, which uses the Hay−Wadt effective core potential (ECP)[21] and basis set for rhodium, and the 6-31G* basis set for all other atoms. Solvation was simulated using a polarized continuum model (PB-SCRF) with parameters suitable for THF,[29] which was deemed sufficiently similar to the ethereal diglyme used in the experimental investigations.[30] In the gas phase, intermediates and transition states were characterized by a full, analytic frequency calculation, which resulted in only positive frequencies for intermediates and exactly one imaginary frequency for the transition states. In all cases, did a visualization of this imaginary frequency correspond to the expected normal mode for the elementary step under investigation.

A theoretical estimation of the kinetic isotope effect was performed using the available Hessian from the full frequency calculation by simply changing the isotope of the aldehydic H atom. To allow comparison to the experimental value, the Gibbs free energies were calculated for a temperature of 440 K.

Acknowledgment. Financial support from the Lundbeck Foundation is gratefully acknowledged. The Center for Sustainable and Green Chemistry is supported by the Danish National Research Foundation. We thank Dr. Fedor Zhuravlev and Dr. Mårten Ahlquist for fruitful discussions.

Supporting Information Available: Detailed experimental procedures, additional kinetic plots along with *XYZ* coordinates, SCF energies, Gibbs free energies (298 and 440 K) for all structures with the full experimental ligand. This material is available free of charge via the Internet at http://pubs.acs.org.

JA710270J

(24) Kaesz, H. D.; Saillant, R. B. *Chem. Rev.* **1972**, *72*, 231–281.
(25) Bigeleisen, J.; Mayer, M. G. *J. Chem. Phys.* **1947**, *15*, 261–267.
(26) Houk, K. N.; Gustafson, S. M.; Black, K. A. *J. Am. Chem. Soc.* **1992**, *114*, 8565–8572.
(27) Singleton, D. A.; Wang, Z. *J. Am. Chem. Soc.* **2005**, *127*, 6679–6685.
(28) For updated versions, see: http://www.schrodinger.com.
(29) (a) Marten, B.; Kim, K.; Cortis, C.; Friesner, R. A.; Murphy, R. B.; Ringnalda, M. N.; Sitkoff, D.; Honig, B. *J. Phys. Chem.* **1996**, *100*, 11775–11788. (b) Tannor, D. J.; Marten, B.; Murphy, R.; Friesner, R. A.; Sitkoff, D.; Nicholls, A.; Ringnalda, M.; Goddard, W. A., III; Honig, B. *J. Am. Chem. Soc.* **1994**, *116*, 11875–11882.
(30) The parameters for THF were used since these have been determined with significantly better accuracy than the corresponding parameters for diglyme. Calculations on the small model system in Figure 11 (L = CO) using parameters for diglyme ($\epsilon = 7.0$, $\rho = 0.94$) gave results which were within 1 kJ/mol of the ones obtained with the parameters for THF.